Interfacial velocities and the resulting velocity field during a Haines jump

R. T. Armstrong[3], N. Evseev[2], D. Koroteev[2], S. Berg[1]

[1]Shell Global Solutions International BV, The Netherlands.
[2]Schlumberger Moscow Research, 13 Pudovkina Street, 119284 Moscow, Russia
[3]School of Petroleum Engineering, University of New South Wales, NSW 2052 Sydney, Australia

ABSTRACT

The movement of immiscible phases through porous media is an ensemble of rapid pore-scale events that occur as interfaces pass through the convergent and divergent pore space. The relevance of these pore-scale events, referred to as Haines Jumps, for larger scale models is often questioned. A common counter argument is that the resulting large fluid velocities would average-out once a bulk representative volume is considered. However, in our opinion this is often stated without direct experimental and/or numerical evidence. In this study, we couple a pore-scale simulation tool with experimental results from a micromodel system equipped with a high speed camera to study Haines jumps at the detail necessary to determine the length scale over which these events influence the bulk velocity field. We first demonstrate that the pore-scale simulation approach, using density functional hydrodynamics (DHD), mechanistically compares well to experimental observations and other well-known displacement processes. Then experimental measurements of fluid-fluid interfacial velocities are used to test the DHD simulator. Simulation results are then used to analyze the local velocity field associated with an individual jump and thus, provide information on the zone of influence associated with a Haines jump. The results of this study demonstrate how interfacial dynamics affect the surrounding velocity field and over what distance this effect is observable. Therefore, the results have direct implications on how system parameters should be averaged when up-scaling from the pore-scale to core-scale.

INTRODUCTION

The pore-scale modeling of multiphase flow through porous media using digital rock images is an area of research in the oil and gas industry with increasing relevance. This technology, often referred to as Digital Rock, has the potential to streamline the special core analysis workflow, facilitate more informed decisions when developing an experimental program, and allow for the evaluation and risk minimization of different enhanced oil recovery technologies. Additionally, as computational capacity and speed increases, the gap between pore-scale and core-scale simulations is narrowing, which

provides an exciting opportunity for pore-to-core scale analysis and new tools for evaluating the up-scaling problem. Bulk system dynamics, such as relative permeability, are commonly measured with pore-scale simulations and the results are often validated against experimental data. Even though good agreement is reported, the predictability of these simulation tools is unclear, i.e. are the correct displacement dynamics captured or is the agreement simply a result of history matching. It is therefore important that any pore scale simulation tool captures the correct pore-scale physics, i.e. the correct displacement mechanisms at the relevant time and length scales must be reproduced. Since the 1970s, observations from pore-scale experiments have been used to identify many important displacement mechanisms, which are described by terms, such as Haines jump, snap-off, piston-like displacement, corner flow, ganglion dynamics and film swelling [2, 17, 19, 20]. Sequentially, these mechanisms have been used to develop mechanistic rules for network models, as explained in [3]. Likewise, for the validation of a pore-scale simulation tool, we wish to decompose the pore-scale physics into the elementary mechanisms [17] and then test the capability of a given modeling tool to correctly capture the dynamics of a given mechanism. By correctly capturing the transient dynamics, we not only instill confidence in the simulation results, we also are able to study the associated length and time scales for a given mechanism, which ultimately set the lower limit for spatial and temporal averages during the up-scaling processes.

In this work, we study the pore-scale displacement mechanism known as a Haines jump [14]. We study the transient dynamics of Haines jumps and link the traditional mechanistic description to measurable pore-scale parameters. A micromodel system equipped with a high-speed camera is used to image transient interfacial dynamics during drainage and the resulting images are used to measure interfacial velocities. These measurements are then used to validate pore-scale simulations of Haines jumps using a modeling tool called the Direct HydroDynamic (DHD) simulator [4]. The results of which also give further consistency to our experimental observations [1]. We then use the DHD simulator to explore the influence of fluid viscosity and interfacial tension on the speed of a Haines jump because this sets a fundamental characteristic time scale for fluid-fluid displacement during drainage. To measure the characteristic length scale associated with a Haines jump, and thus, the zone over which interference could occur between simultaneous jumps, we use the DHD simulator to extract the phase velocity vectors during a Haines jump. The results provide a clearer link between a mechanistic displacement process and quantifiable pore-scale parameters that define the length and time scales of a Haines jump, which has consequences when defining a representative elementary volume (REV) and when performing pore-scale simulations.

METHODS AND MATERIALS

Experimental System

The experimental system was explained in [1]. For convenience, we only repeat the most relevant details. The borosilicate glass micromodel was chemically etched with a hexagonal pattern (depth = 5 μm, pore diameter = 60 μm, and neck width = 13 μm), see

Figure 1. Pore drainage events were imaged at 2000 frames per second (fps) using an inverted transmission microscope equipped with a high speed camera. The wetting phase was Millipore water and the non-wetting phase was decane [1]. The flow rate was controlled with a syringe pump, which allowed for constant flux boundary conditions. The experimental parameters are presented in Table 1, as Case 1.
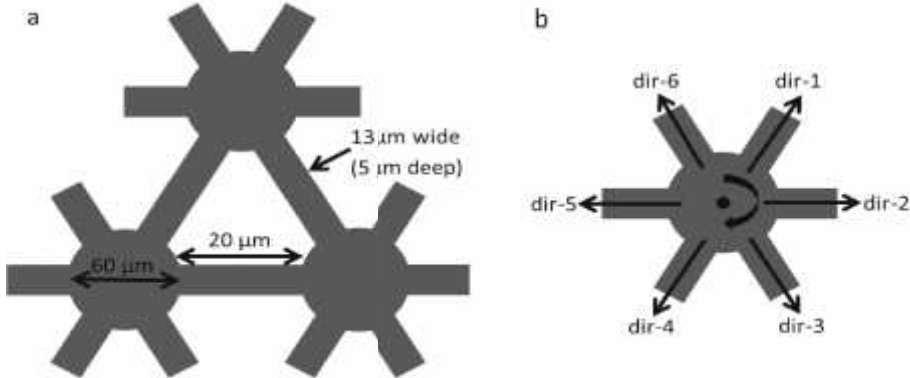

Figure 1: Hexagonal model geometry (not to scale) used in the presented simulations and experiments (a). Line profiles used for investigating the velocity field during a Haines jump.

Table 1: Parameters tested with the DHD simulation tool. Case 1 is the baseline case, for all other cases either the viscosity or the interfacial tension was increased or decreased by an order of magnitude.

Case (#)	Interfacial Tension (N/m)	Oil viscosity (Pa·s)	Flux (m³/s)	Velocity (m/s)	Contact angle (°)	Ca_{micro} (-)
1	0.029	9.2E-04	1.17E-12	6.5E-04	50.4	3.26E-05
2	0.029	9.2E-04	4.69E-12	2.6E-03	50.4	1.30E-04
3	0.029	9.2E-04	1.17E-11	6.5E-03	50.4	3.26E-04
4	0.029	9.2E-05	1.17E-12	6.5E-04	50.4	3.26E-06
5	0.029	9.2E-03	1.17E-12	6.5E-04	50.4	3.26E-04
6	0.144	9.2E-04	1.17E-12	6.5E-04	82.6	3.24E-05
7	0.003	9.2E-04	1.17E-12	6.5E-04	0	2.08E-04

A matrix of the parameters tested with the DHD simulator is presented in Table 1. Case 1 is the baseline from which either interfacial tension, viscosity, or flow velocity is varied. Each variable is increased or decreased from its baseline value while all other parameters remain constant. We also computed the microscopic capillary number $Ca_{micro}=\mu v/(\sigma\cos(\theta))$ (where, μ is viscosity, v is average pore velocity, σ is interfacial tension, and θ is contact angle) in order to assess whether the displacement patterns are similar for the same Ca_{micro} or whether the actual magnitude of the independent parameters μ, v, σ, or θ matter. The mobility ratio is M is the ratio of displaced and displacing phase, i.e. $M=0.9$ and $\log(M)\sim0$. for the case of n-decane displacing water in drainage [1].

Interfacial velocities were measured with Tracker [4]. Prior to a Haines jump the three phase contact point remains pinned at the entrance to a pore body and the decane/water interface "bulges" into the pore body where according to the Laplace equation the increase in curvature visually represents the increase in pressure in the non-wetting phase. At this point, a reference line that is normal to the interface and extends diagonally across the pore body can be drawn by visually examining an image. Once the pore entry pressure is exceeded the interface accelerates through the pore body and the movement is tracked along the reference line. From this analysis, the speed (velocity magnitude) of the oil/water interface during a Haines jump is measured. To visualize the simulation results and thus, fluid velocities the magnitude of the x and y velocity vectors were mapped to color images. Then, velocity profiles along lines that extend outward from the center of a pore from which a Haines jump occurs are reported. The direction and numbering of these line profiles are provided in Figure 1b.

Numerical Simulator
We use the method of Density Functional Hydrodynamics (DFH), which consists of both a hydrodynamic and thermodynamic model that are coupled through the conservation laws of mass and momentum [9]. At this juncture, we only provide reference material that explains DFH since the establishment and validation of this method has progressed through a series of papers since 1995 [7-13]. The up-to-date description of the accumulated results as well as the information on the hydrodynamic and thermodynamic models, and numerical technique called Tensor-Aligned Conservative Uniform Symmetric (TACUS) used for solving the new system of equations arising in DFH are all described in the book [6]. The Direct HydroDynamic (DHD) simulator solves the DFH equations by the TACUS method on either CPU or GPU-based computer clusters. This simulator has been used to model various pore-scale multiphase flow mechanisms applied in practical industry applications [15, 16].

RESULTS AND DISCUSSION
As shown in Figure 2, the simulation results are very similar to (previously published [1]) experimental observations. In both the experiment and the simulation, during a Haines jump when a pore body is filled, menisci in adjacent pore throats retract [1]. This effect points to the insight that the transient pore drainage dynamics are not only controlled by the global pressure field exceeding the local capillary entry pressure to the pore body, but rather by a capillary pressure (P_c) difference between the heading meniscus in the pore body (black arrow) and the trailing menisci, i.e. the menisci in the vicinity (red arrow). This suggests that in the context of pore drainage, capillarity is a non-local process that depends on the entry pressure of a single pore and also the fluid topology in the vicinity.
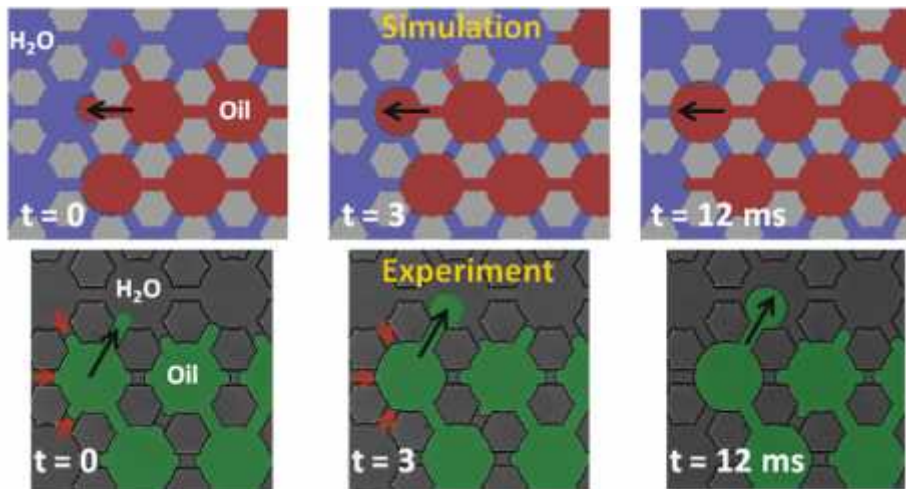
Figure 2: The simulation results display the same cooperative pore drainage patterns as observed in the experiments reported in [1].
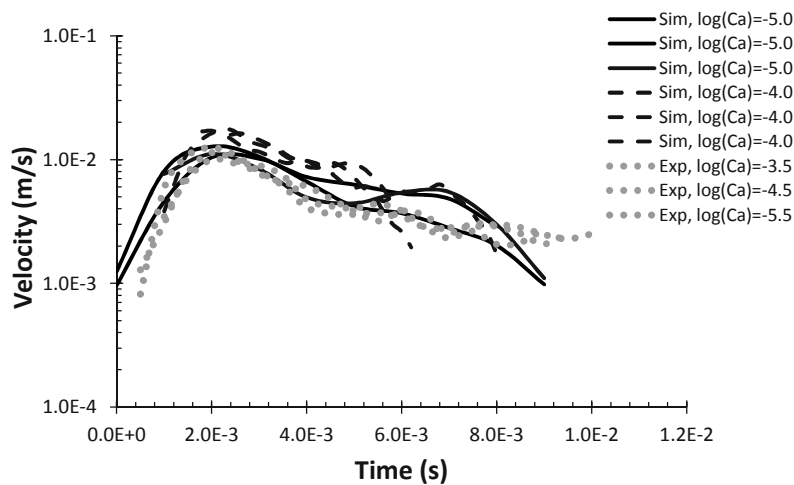

Figure 3: The measured interfacial velocities for the experimental data are independent of bulk flow rate, reported as a change in capillary number (Ca). The simulation results display the same independency.

In both the experiment and the numerical simulation, pores are drained in approximately the same time scale, as shown in Figure 3. The interface accelerates for the first 2-3 ms and then decelerates until fluid comes to a rest after 10-12 ms. This sets an intrinsic time scale that is independent of bulk flow rate (except for high bulk flow rates where the flux is larger than that of individual pore filling events [1]). These results suggest that the simulator is correctly capturing the transient dynamics of individual pore drainage events and the cooperative dynamics between individual events, which increases our confidence that also more complex flow patterns that are necessary for modeling multiphase flow in

a porous medium are correctly represented. It is important to note that the flow velocities during Haines jumps are significantly larger than the assumption of creeping flow on which Darcy's law is based. Here we measure flow velocities up to 0.1-1 m/s, which translates to Reynolds numbers of the order of 1. This means that pore-scale simulators need to consider the full Navier-Stokes equation and not just Stokes flow to capture the correct fluid-fluid displacement dynamics.

With this validation we can use DHD to explore how sensitive the displacement dynamics are to changes in basic parameters. From the results displayed in Figure 4, we find that interfacial velocities depend on viscosity and interfacial tension.
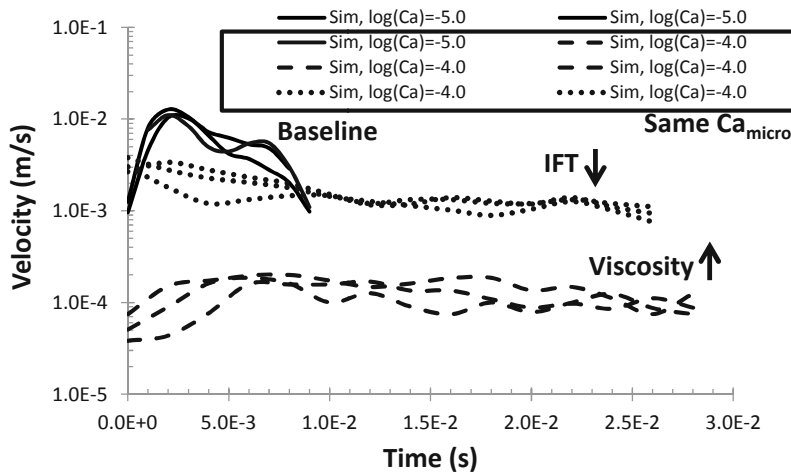

Figure 4: Simulation results indicate that interfacial velocities are dependent on the viscosity of the invading phase and the interfacial tension between immiscible phases, reported as a change in capillary number Ca_{micro}.

As displayed in Figure 4, we observe that the time scale for a pore drainage event can be affected: it increases with increasing viscosity and decreases with decreasing interfacial tension (Figure 5).
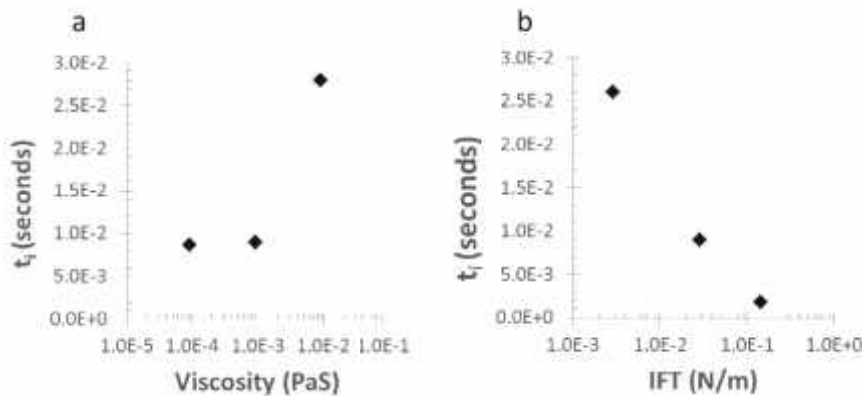

Figure 5: The time scale for a pore drainage event increases with increasing viscosity (a) and conversely it decreases with decreasing interfacial tension (b).

Please note that for some of the cases (see Table 1) we keep $\mu v/\sigma$ constant e.g. by increasing viscosity of the displacing phase by a factor of 10 and decreasing interfacial tension by a factor of 10. Nevertheless, the displacement patterns are different for the two cases which clearly indicates that $Ca_{micro}=\mu v/(\sigma\cos(\theta))$ is not the only parameter characterizing the displacement. Since the viscosity of the injected phase was changed, also the mobility ratio $M=\mu_2/\mu_1$ of displacing and displaced phase changes. Lenormand *et al.* [18] have parameterized the displacement regimes with the parameters capillary number (Ca) and mobility ratio M. In Figure 6, we compare our displacement regimes with the stability diagram of Lenormand and find an overall good agreement with the general trends suggested by the phase diagram.
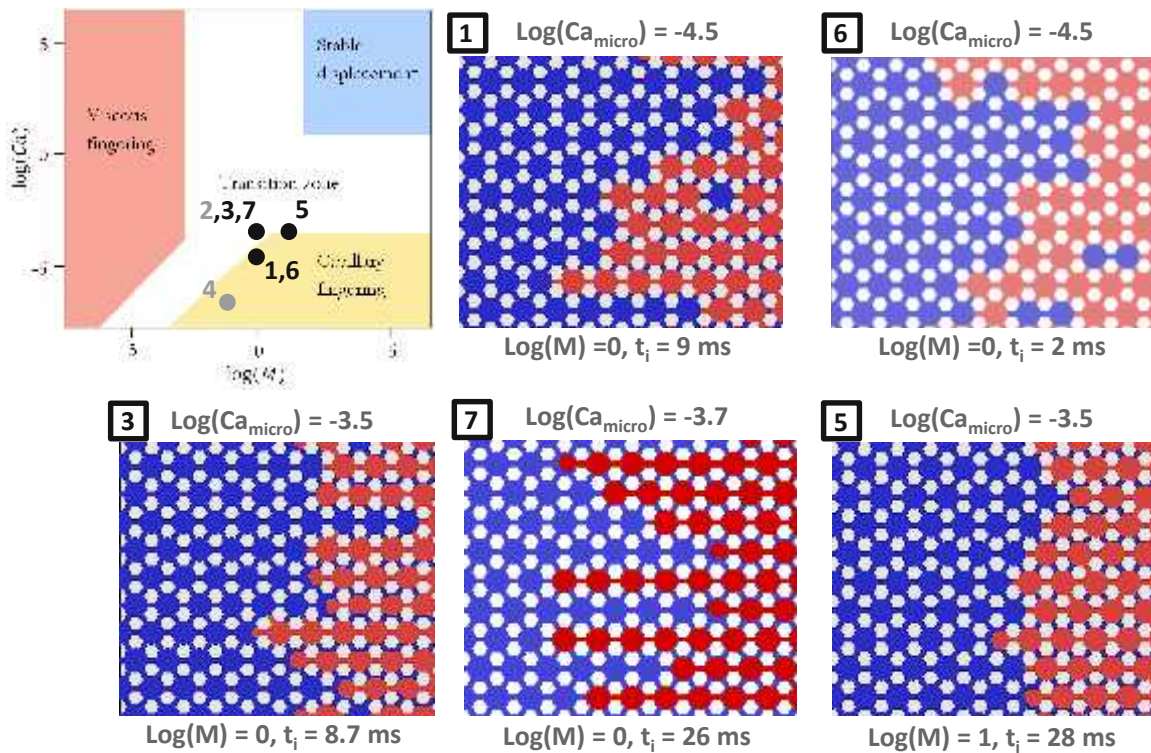

Figure 6: The flow regime, i.e. the characteristics of the displacement, is controlled by both capillary number Ca_{micro} and mobility ratio M. The cases from Table 1 are consistent with the flow regimes observed by Lenormand *et al.* [18].

We also have to realize that according to the Young equation, changes in interfacial tension σ_{ow} between oil and water also implies a change in the contact angle

$$\cos\theta = \frac{\sigma_{so} - \sigma_{sw}}{\sigma_{ow}}$$

with σ_{os} and σ_{ws} being the oil-solid and water-solid interfacial energies, respectively. Therefore the capillary number should indeed include the contact angle

$$Ca_{micro} = \frac{\mu \cdot v}{\sigma \cdot \cos\theta}$$

Decreasing σ_{ow} by a factor of 10 also decreases a contact angle from e.g. initially 50° to practically 0° which means that a system where the oil is partially wetting, i.e. with a joint contact line between water, oil and solid, becomes completely non-wetting for the oil. As a consequence, the water films become continuous which is a more conceptual change for the displacement pattern, as displayed in Figure 7.
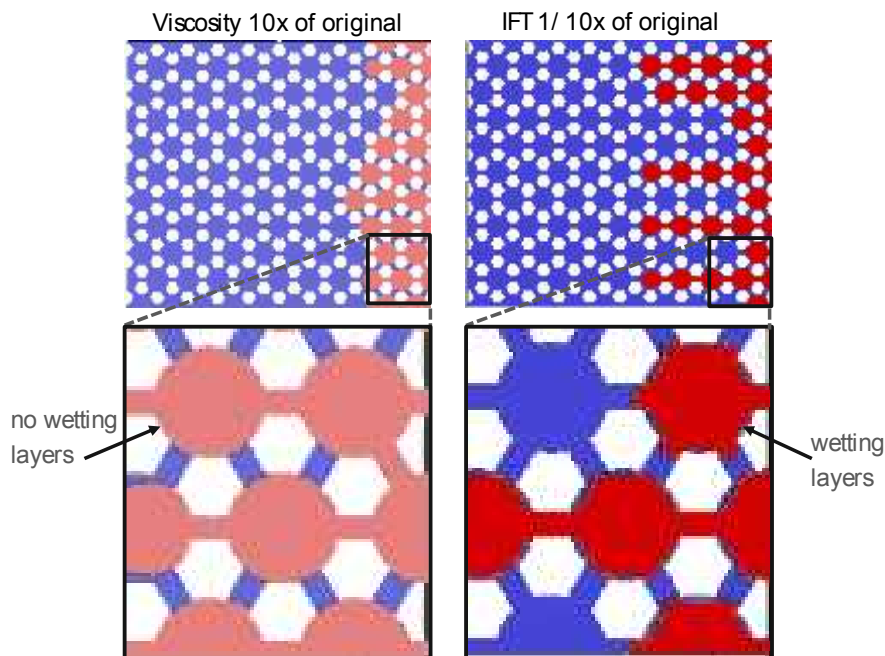

Figure 7: Conceptual difference between changing viscosity (case 5, left) and interfacial tension (case 7, right). For the increase in viscosity in case 5, the contact angle remains the same, as in the case 1. But when decreasing in case 7 the interfacial tension by a factor of 10, the contact angle becomes practically 0° which leads to stable wetting films and a very different displacement pattern.

For many considerations, e.g. estimating the viscous and inertial forces in relation to the capillary forces for a pore drainage event it is important to include the total fluid in motion and not only the fluid in the pore that is drained. Already in the comparison between experiment and numerical simulation, displayed in Figure 2, we have observed that the cooperative effects of pore drainage events involve neighboring pores up to several pores away. From these observations a few interesting questions arise:
(1) Over what spatial distance do these drainage events actually interact?
(2) Likewise, for both the displacing and displaced phase, how big is the zone of influence of a pore drainage event.

From the experiments, this is difficult to measure because we cannot directly observe the flow field but can only indirectly infer on flow velocities via the motion of menisci. From the numerical simulation, which we have validated against experimental data in Figure 2 and Figure 3, we have obtained a flow field.
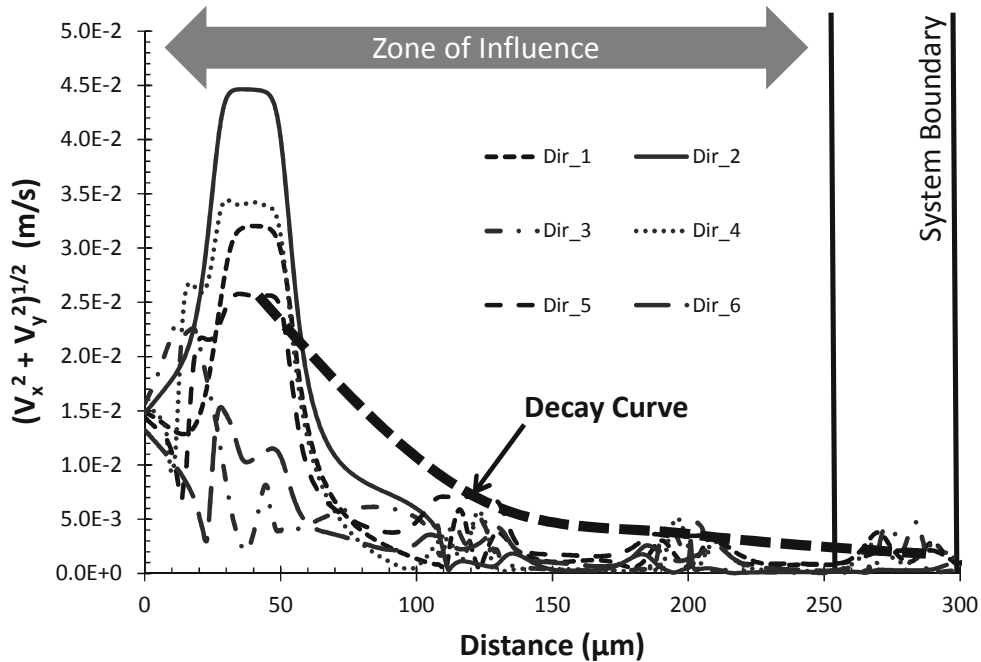

Figure 8: Velocity profiles for Case 1. Measurements were taken along line profiles that extend outward, from the center of a pore from which a Haines jump occurs, in the 6 radial directions (Dir) that correspond to the hexagonal model geometry (see Figure 1b). Line profile measurements are reported for the maximum interfacial velocity reached during a jump.

By measuring the fluid velocity magnitude along the lattice direction of our porous pattern (Figure 1), we observe the decay of the velocity field from the pore, as shown in Figure 8. Note that the flow velocity does not decrease monotonically but shows local maxima that correspond to the pore throats because of the conservation of momentum and the continuity equation (lower flow velocity in the wider pore bodies and higher velocity in the narrower pore throats). Here we estimate the zone of influence by assessing the decay of the flow field in the pore throats and set the zone of influence to the point where the measured velocities are similar to the predict Darcy velocity. For the Case 1 example in Figure 8, we observe decay over a distance of about 4 pores, which means that the total zone of influence is about 8 by 8 pores. When increasing the viscosity (Case 5) the zone of influence decreases to about 2-3 pores and when increasing the interfacial tension (Case 6) the zone of influence increases beyond the boundary of the modelling domain. While these results are for a 2D system the observed trends should hold for a 3D porous rock.

CONCLUSIONS

In two-phase flow in porous media it was observed that pore drainage events are cooperative processes where the heading meniscus in the draining pore body interacts with multiple trailing menisci in adjacent pores. This leads to complex transient dynamics that was observed both in experiments and in the numerical modelling study. We used the pore scale simulator called Direct HydroDynamics (DHD), which is based on an approach, in which thermodynamic and hydrodynamic models along with the diffuse interface approach are implemented via a density functional formulation. The transient dynamics of pore drainage events observed in micromodel experiments were reproduced by DHD in all its complexity: the general behavior with cooperative drainage events and the time scale of drainage events were in good agreement. At the pore-scale, drainage events are rapid: they last only few milliseconds with flow velocities up to 0.1-1 m/s and Reynolds numbers of the order of 1. This confirms that multiphase flow is not a low Reynolds-number flow and implies that numerical simulators need to consider the full Navier-Stokes equation.

Following the validation, DHD was used to investigate properties and parameter variation, which experimentally are not easily accessible. A parametric study where interfacial tension and viscosity of the injected phase were systematically varied showed significantly different interfacial dynamics occur for the same microscopic capillary number. These results suggest that the microscopy capillary number is not sufficient to characterize the transient dynamics and the associated pore scale flow regimes.

By using the velocity field computed by DHD the zone of influence of a Haines jump was estimated to range over several (up to 5-by-5) pores. Within this zone of influence, (and probably also beyond) which is clearly larger than the single-phase representative elementary volume in this 2D system (which would be here one lattice unit, i.e. one single pore), the pressure fluctuations do not average out. Therefore, the spatial density of such jumps in a 2D system, such as ours, should be less than 1 event per 25 pores. This analysis is likely to change for a 3D system; however, the overall concept that the spatial density of pore-scale events should be considered when defining an REV, i.e. the dynamics must be considered, has not been addressed elsewhere. The importance of this point is often overlooked when modeling or experimental studies are performed on a single pore/junction or small field of view.

The ability to compute pore scale transient displacement accurately provides access to a multitude of important parameters. The flow field and knowledge on the zone of influence is useful to compute pore scale force balances like the magnitudes of the capillary, viscous, and inertial forces. For both viscous and inertial forces it is required to consider the total fluid at motion and not only the fluid in a single pore. This work performed on a 2D system provides the foundation to study similar effects in 3D pore geometries of real rock. By considering more complex and larger geometries up to realistic pore structures a more detailed analysis of phenomena like the capillary dispersion zone which is within the Darcy-scale range and the disperse boundary between the water and oil in an unsteady-state displacement becomes feasible.

ACKNOWLEDGMENTS

REFERENCES

*   Corresponding author; E-mail address: steffen.berg@shell.com

1. Armstrong, R. T. and S. Berg (2013), Interfacial velocities and capillary pressure gradients during Haines jumps, *Physical Review E*, 88(4).
2. Avraam, D. G. and Payatakes, A. C. (1995), Flow regimes and relative permeabilities during steady-state two-phase flow in porous media, *Journal of Fluid Mechanics*, 293, pp 207-236.
3. Blunt, M. J. (2001), Flow in porous media – pore-network models and multiphase flow, Current Opinion in Colloid and Interface Science 6(3), pp. 197-207.
4. Brown, D., Video Modeling with Tracker, AAPT 2009 Summer Meeting, 29 July 2009
5. Demianov, A., Dinariev, O., and N. Evseev (2011), Density functional modeling in multiphase compositional hydrodynamics, *Canadian Journal of Chemical Engineering*, 89, 2, pp 206-226.
6. Demianov, A., Dinariev, O. and N. Evseev (2014), Introduction to the density functional method in hydrodynamics. Fizmatlit, Moscow, ISBN 978-5-9221-1539-1.
7. Demyanov, A. and O. Dinariev (2004), Modeling of Multicomponent Multiphase Mixture Flows on the Basis of the Density Functional Method, *Fluid Dynamics* 39, 6, pp 933–944
8. Demyanov, A. and O. Dinariev (2004), Application of the Density-Functional Method for Numerical Simulation of Flows of Multispecies Multiphase Mixtures, *Journal of Applied Mechanics and Technical Physics* 45, 5, pp 670-678.
9. Dinariev, O. (1995), A Hydrodynamic Description of a Multicomponent Multiphase Mixture in Narrow Pores and Thin Layers, *Journal of Applied Mathematics and Mechanics*, 59(5), pp 745–752.
10. Dinariev, O. and N. Evseev (2005), Description of the Flows of Two-Phase Mixtures with Phase Transitions in Capillaries by the Density-Functional Method, *Journal of Engineering Physics and Thermophysics*, 78, 3, pp 474-481.
11. Dinariev, O. and N. Evseev (2007), Description of viscous-fluid flows with a moving solid phase in the density-functional theory, *Journal of Engineering physics and Thermophysics*, 80, 5, pp 70-77.
12. Dinariev, O. and N. Evseev (2007), Application of density-functional theory to calculation of flows of three-phase mixtures with phase transitions, *Journal of Engineering physics and Thermophysics*, 80, 6, pp 1247-1255
13. Dinariev, O. and N. Evseev (2010), Modeling of Surface Phenomena in the Presence of Surface-Active Agents on the Basis of the Density-Functional Theory, *Fluid Dynamics*, 45, 1, 85–95
14. Haines, W. B. (1930), Studies in the physical properties of soil. V. The hysteresis effect in capillary properties, and the modes of moisture distribution associated therewith, *The Journal of Agricultural Science*, 20(97), pp. 97-116.
15. Koroteev, D., Dinariev, O., Evseev, N., Klemin, D., Nadeev, A., Safonov, S., Gurpinar, O., Berg, S., van Kruijsdijk, C., Armstrong, R. T., Myers, M. T., Hathon, L. and H. de Jong (2013), Direct hydrodynamic simulation of multiphase flow in porous rock, *SCA2013-014*, Napa Valley, California, USA.

16. Koroteev, D., Dinariev, O., Evseev, N., Klemin, D., Safonov, S., Gurpinar, O., Berg, S., van Kruijsdijk, C., Myers, M., Hathon, L. and H. de Jong (2013), Application of Digital Rock Technology for Chemical EOR Screening, *SPE-165258*.
17. Lenormand, R., Zarcone, C., and A. Sarr (1983), Mechanisms of the displacement of one fluid by another in a network of capillary ducts, *Journal of Fluid Mechanics*, 135, pp. 337-353.
18. Lenormand, R, Touboul, E, Zarcone, C, (1988), Numerical models and experiments on immiscible displacements in porous media, *Journal of Fluid Mechanics*, 189, 165-187.
19. Mohanty, K. K., Davis, H. T., and L. E. Scriven (1987), Physics of oil entrapment in water-wet rock, *SPE Reservoir Engineering*, SPE 9406, pp. 113-128.
20. Morrow, N. (1969), Physics and thermodynamics of capillary, *Industrial and Engineering Chemistry*, Flow Through Porous Media Symposium, pp. 32-56.